2012

TECHNICAL REPORT LMR-03

TECHNIQUES FOR ROCK PERMEABILITY DETERMINATION I. STEADY STATE FLOW, PULSE DECAY AND PORE PRESSURE TRANSMISSION METHODS

UNIVERSIDADE DA CORUÑA

CITEEC
Research Center for Technological Innovations in Construction and Civil Engineering

CREDITS

This report has been elaborated by Ismael Falcón and revised by Jordi Delgado, Jacobo Canal, Víctor Barrientos & Ricardo Juncosa. For citation purposes, please use the following information: *Falcón, I. 2012. Techniques for rock permeability determination I. Steaty state flow, pulse decay and pore pressure transmission methods. LaMeRoc Technical Report LMR-03; 21 pp.*

INDEX

1. Introduction

Permeability is an intrinsic property of porous media that can be easily characterized in many instances through the measurement of the steady flow rate associated to a given pressure gradient. For the measurement of permeability in highly connective porous media, the steady state flow rate method (SSFM), which is based on the direct application of the Darcy´s law, is straightforward provided that an accurate control on the geometric properties of the tested specimen is known and a careful monitoring of pressure and flow. However, its application to low permeability, tight rocks, still represents a challenge due to the significantly longer equilibration times needed to attain the steady-state condition or the difficulty in guarantee the stability in certain physical properties of the tested sample (pore volume change in soft materials) or the accuracy of measuring devices in extremely low flow conditions. Transient methods constitute a workable alternative to the traditional steady-state technique. Worth mentioning among them are the so called pulse decay (Brace et al., 1968; Jouniaux *et al.*, 1994) and the pore pressure transmission (Metwally and Sondergeld, 2011) methods (PDM and PPTM, respectively). The practical implementation of transient techniques for measuring permeability is not straightforward and a number of issued must be solved before obtaining meaningful data.

The purpose of this report is to illustrate the implementation of the PDM and PPTM transient methods at the LaMeRoc and to test them against the SSFM. The three methods have been applied to low permeability plugs of granite (~300 nD or ~$3x10^{-19}$ m^2). It is not the purpose of this report to perform a complete review of the available literature concerning transient methods for permeability measurements and only a few details will be given in order to better understand the procedures employed.

2. Experimental Rig

Permability measurements were performed using an experimental ring composed by a high pressure core holder and different hydraulic pumps. The core holders used were specific to work with 1.5’ (38.1 mm) diameter rock plugs. Core holders used were a modified Hoek-Franklin-type (Hoek and Franklin, 1968) and RCHT-series, Hassler-type (Hassler, 1944) fabricated by Core Labs Instruments (Fig. 1). The main difference between them is the absence of stainless-steel compression platens to load the axial stress, in the case of Hassler cell. However, both cells can triaxially pressurize the rock specimen to test it for permeability (Hoff and Hall, 2002).

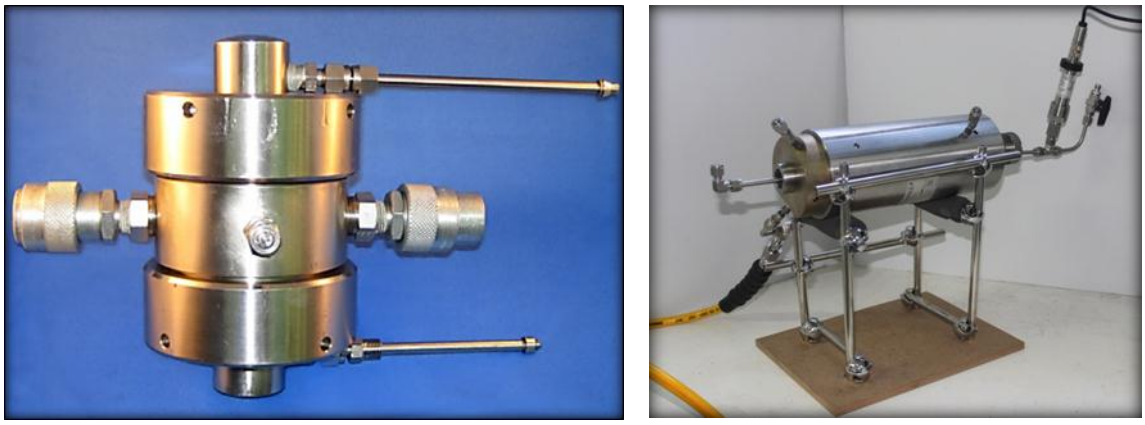

Figure 1. ***Left.*** Modified Hoek-Franklin-type core holder. ***Right.*** RCHT-series, Hassler-type core holder.

Confining and axial pressure for both configurations were provided by two independent ENERPAC Series P hand hydraulic pumps equipped with check valves to set and hold the pressure, and analogic gauges for monitoring. Pore pressure was delivered through a high-pressure, high-resolution fluid injection system Quizix SP-5400 which has four cylinders, paired two to two (Fig. 2). The Quizix system allows the pulseless injection of fluids up to a pressure of 79 MPa, with a volume resolution of 0.31 nL.

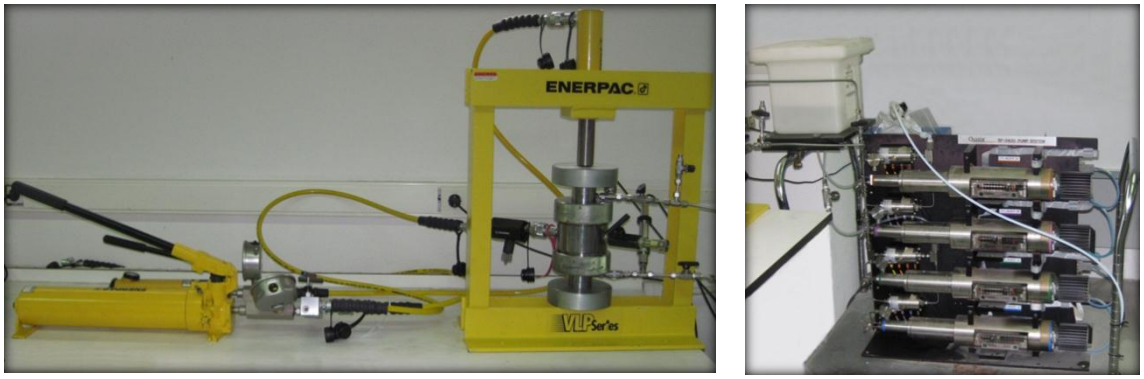

Figure 2. ***Left.*** ENERPAC Series P hand hydraulic pumps and load frame equipped with a Hoek-Franklin core holder. ***Right.*** The Quizix SP-5400 fluid injection system.

The Quizix system can be programmed for a wide number of operations and sequences using the PumpWorks software (Chandler Engineering). This software is able to graphically display the instantaneous record of pressure and temperature corresponding to internal pressure transducers and to collect and store data (data acquisition system). The main purpose of Quizix system is to pressurize and transfer a fluid (de-aireated water, brine, kerosone, etc.) from an external reservoir to the porous space of the rock plug using a high pressure stainless steel pipe, valves and connectors. Acting in a paired way, two Quizix cylinders can work as deliver (downstream) reservoirs while the other two remain as receiver (upstream) reservoir. The pressure in

the up and downstream reservoirs can be preset or left to change up to achieve some certain target value.

In addition to the pressure transducers installed in the Quizix pumps, two accurate absolute pressure transmitters (Keller-Drück LEO Record Ei) have been in the corresponding tees up and downstream the rock sample (Fig. 3A). Both transmitters are connected to a data acquisition system. This system provides with a redundant pressure gradient check which is important to evaluate the accuracy of the experimental system. Apart from the valves implemented in the Quizix system, the rig is equipped with only four extra high pressure manual valves (1 to 4 in Fig. 3): two upstream and two downstream the core holder. This configuration makes possible to split the entire system into six smaller reservoirs (V_1 to V_6). In order to prevent temperature effects over fluid compressibility for low permeability samples, a thermal chamber was constructed around the rig (core holder + pipes & accessories + Quizix) to isolate it from external fluctuations on long lasting experiments.

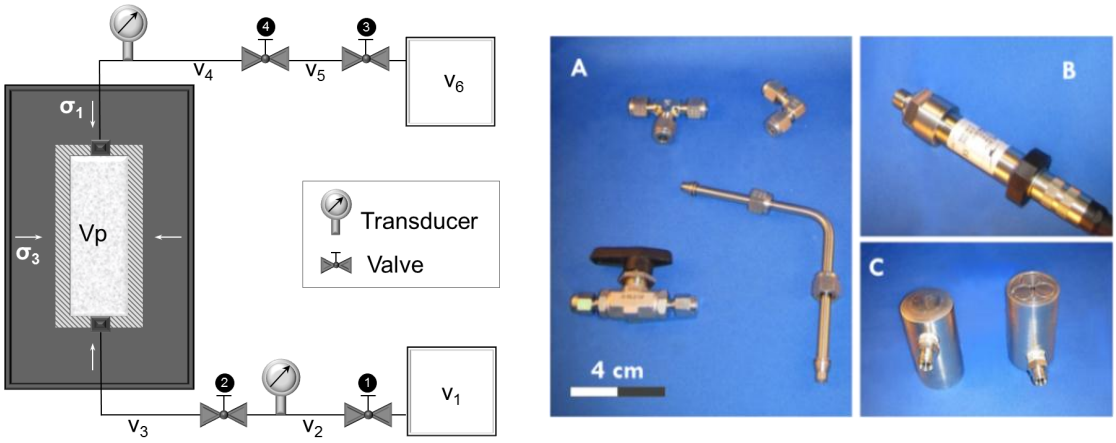

Figure 3. ***Left***. Conceptual sketch ilustrating the main features of the experimental rig used. V_1 and V_6 represent the up and dowstream reservoirs, respectively (each one associated to a pair of Quizix cylinders). V_2, V_3, V_4 and V_5 represent the volumes associated to different sections of the fluid circuitry (the sum of pipe internal volume, load platen groove volume and dead volumes of valves and pressure transmitters). V_P corresponds to the pore volume of the rock plug. ***Right***. Different accessories used in the experimental system: A, steel pipes, valves and tee & elbow-type connectors; B, Keller-Drück LEO Record Ei absolute pressure transmitter; C, grooved load platens.

3. Materials and Methods

So far, permeability measurements have been developed using the SSFM, PDM and PPTM methods with a number of different samples. In this report we present results associated to the same core plug tested using the three previously mentioned approaches. The comparison between the three methods allow us to state the accuracy of the permeability determination as well as to get some ideas about the

sensitivity with respect the determination of certain parameters, all of them critical for the application of transient (PDM, PPTM) techniques.

The rock samples used may be called *opportunity samples*, *i.e.* those available in the lab without making question of other property than that important for the tests being performed. Accordingly, we worked with either natural (igneous & metamorphic rocks) or artificial (cement) plugs with the single specification of having apparent homogeneity, low porosity and low to very low permeability. It is acknowledged that more rigorous selection criteria should be followed on a general basis. However, for the preliminary nature of the works performed, that was considered satisfactory for demonstration purposes.

Plugs were carefully cored from the original rock (casted in a PVC mould of adequate diameter and left to cure at moisture saturation in a climatic chamber, in the case of cement) and then trimmed to fulfil standard geometric constrains for rock mechanics studies: flatness, slenderness and cylindricity tolerances (Fig. 4). Then, the sample plugs were oven-dried (24 hours), weighted and its dimensions verified in order to determine basic physical properties (dry density, specific weight).

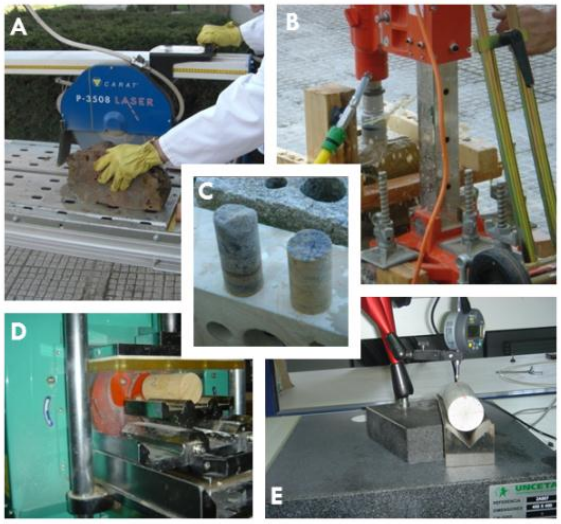

Figure 4. Photographic summary of sample preparation procedure: A, rock block size reduction; B & C, core plug extraction; D, plug trimming; E, verification of the dimensional compliances of the core plug.

Prior to the tests, the sample was step-wise saturated with water using an immersion/suction technique aimed at avoiding the entrainment of air pockets into the sample pore volume. In short, the technique consists in pouring a certain amount of water in a small tray where the sample is located and wait for one day for the capillary rise of water in the sample. Then the water level of the tray is raised to the observed saturation front in the sample and so on up to reach the complete immersion

of the sample. Once the samples were saturated, their weight was recorded again in order to compute the volume of accessible voids from the weight difference with respect the dry sample.

It is interesting to note that the fluid used to saturate the sample (or to inject through it) must be deaerated in order to minimize the effect of mechanically mixed air in the compressibility of the fluid. When measuring low permeability samples, this effects turns out to be relevant, in particular when large pressure gradients may led to air decompression inside voids of the sample. In order to deareate water, we used a commercial Nold 2100 DeAreator (Fig. 5).

Figure 5. *Left.* Nold 2100 DeAreator; *Right.* Room temperature in which is placed the experimental rig.

Prior to the development of any test, saturated samples are emplaced in the corresponding core holder and then pressurized to some preliminary confining and axial pressures. Pore pressure is progressively increased then at the inlet port in order to stimulate water flow. Finally, a constant pressure is imposed upstream while downstream the circuit remains open until outflow is observed. The purpose of this procedure is to drain any air bubble potentially remaining in the conduits which could affect the measurements later performed. From hereafter, the whole circuit is closed and the system is pressurized to the target axial and confining stresses. Then, pressure sensors (transducers) can start logging data.

1.1 Steady State Flow Method (SSFM)

The steady state flow method is based on Darcy´s law. In short, the ratio of volumetric flow rate, Q (m^3 s^{-1}), to the pressure drop, ΔP (Pa), between the inlet and outlet of a sample of cross sectional area, A (m^2), and length, L (m), for a dynamic

viscosity of the fluid, μ (Pa s), is related with its intrinsic permeability, k (m^2), through the following expression:

$$k = \frac{\mu L Q}{A \Delta P} \qquad \text{e.1}$$

A typical test consists of imposing a pressure gradient between the inlet (upstream) and outlet (downstream) of the sampling while monitoring the instantaneous and time-integrated flows at both sides of the sample in order to check for the steadiness condition; it is also valid to prescribe a certain flux value while monitoring pressures at both up- and downstream sides of the sample. The test is typically repeated a certain number of times changing the pressure gradient ($P_{in}+P_{out} \neq$ constant) while keeping the average pore pressure constant ($(P_{in}+P_{out})/2$=constant; see 06). The steady state condition can be evaluated from the slope of the curve cumulative volume *vs.* time by which a constant value represents a constant water flux. Once this condition is verified, permeability can be easily computed from equation e.1. It is worth noting that μ depends on the temperature. Therefore, the value of μ needs to be corrected for temperature taking into account the thermal records associated to the same time period.

The straightforwardness as well as the simplicity in its interpretation makes the SSFM method a good candidate for benchmarking the performance of the alternative, transient methods. However, for the practical application in the laboratory, this method is burden by the long times involved in the careful measurement of low permeability samples.

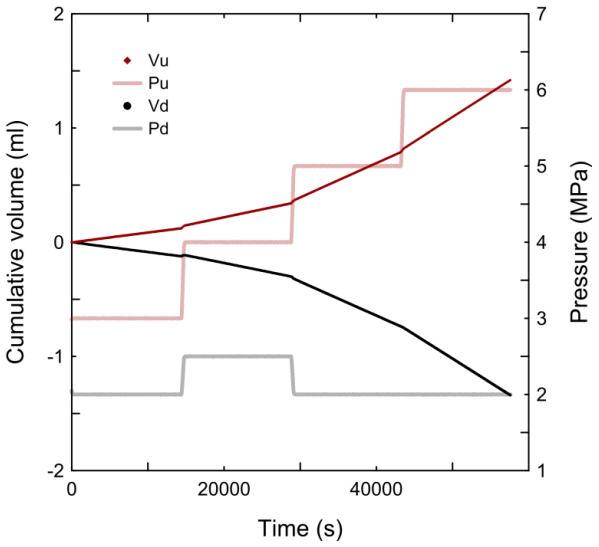

Figure 6. Example of application of the SSFM method to a granite sample submitted to a hydrostatic pressure of 20 MPa and different pressure gradients (i.e., difference between up- and downstream pressures: $P_u - P_d$). V_U and V_d represent water volumes at the inlet and outlet, respectively.

1.2 Pulse Decay Method (PDM)

This method was first proposed by Brace *et al.* (1968) and it has been used widespread to determine the hydrodynamic properties of low permeability media (Boulin *et al.*, 2012; Bourlange *et al.*, 2004; Cui *et al.*, 2010; Jouniaux *et al.*, 1994; Reuschle, 2011). The technique is based on the transient state induced in a porous media (the rock plug) when the equilibrium state is perturbed by suddenly setting a pressure gradient in the sample. Typically, the upstream pressure (P_u) is increased while downstream pressure (P_d) remains unchanged ($\Delta P_0 = P_u - P_d$). Upon perturbation, both up- and downstream pressures evolve with time ($\Delta P(t)$) following an inverse exponential trajectory (transient state) in their natural seeks for the restoration of an apparent equilibrium condition (*i.e.* steady state). The time needed by the system to restore the apparent equilibrium condition depends on the dimensions of the sample and its properties, the volumes of the up- and downstream reservoirs (V_u, V_d), the physical characteristics of the fluid and the pressure gradient imposed (ΔP_0).

$$\Delta P(t) = \Delta P_0 \frac{V_d}{V_u + V_d} e^{-\alpha t} \qquad \text{e.2}$$

where α, represents a decay time constant, further defined in equation e.3 which is function of permeability, the dynamic viscosity of the pore fluid at temperature of measurement, the geometric properties of the sample and the compressive storage of the upstream (C_u) and downstream (C_d) reservoirs. Here, the concept of reservoirs in includes the internal volume of pipes and the dead volumes of transducers, valves, etc.

$$\alpha = \frac{Ak(C_u + C_d)}{\mu L C_u C_d} \qquad \text{e.3}$$

C_u and C_d are defined as the ratios of the change of fluid volume to the corresponding pore pressure variation ($C = \Delta V / \Delta P$). They can be understood as device-specific properties that depending on the material properties and design of all the physical elements contributing to the volume through which the fluid is compressed. Therefore, they represent lumped parameters in which the volumetric response upon compression integrates the behaviour fluid and technological material (steel pipes, compliances of valves, etc.) elements.

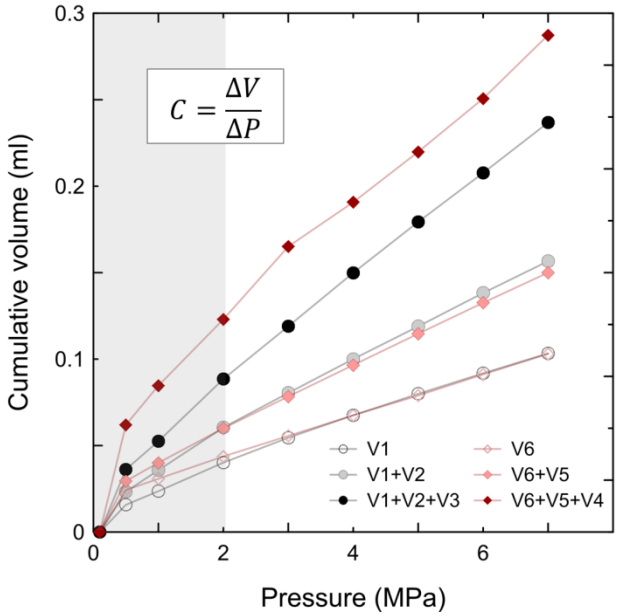

Figure 7. Compressive storage coefficients of each stretch of the hydraulic circuit shown in Figure 3.

These parameters must be assessed experimentally on a local basis (*i.e.* for each laboratory and, in each laboratory, for each experimental configuration). Once they have been assessed, these properties are constants that do not need to be re-assessed unless changes are introduced in the experimental configuration (for instance, a change in the diameter of the steel pipes, etc.).

Figure 7 shows the compressive storage curves of the six sections in which the experimental system constructed can be split. We can observe that, above 0.5 MPa, the curves become linear, being the slope the compressive storage of each section of the circuit.

A critical aspect for the successful application of the PDM is the correct assessment of the relative magnitude of the pressure gradient, ΔP_0. Since both fluid viscosity and compressibility vary with pressure, P_u and P_d cannot depart from a certain value in order to prevent the corresponding gradients within the sample. In addition, permeability greatly depends on the effective confining pressure (P_e), which is defined as $P_e = P_c - P_{u,d}$. Thus, since it was argued by Brace *et al.* (1968), is widely accepted that ΔP_0 should not be higher than a few per cent of P_c and, typically less than 10% of $P_{u,d}$.

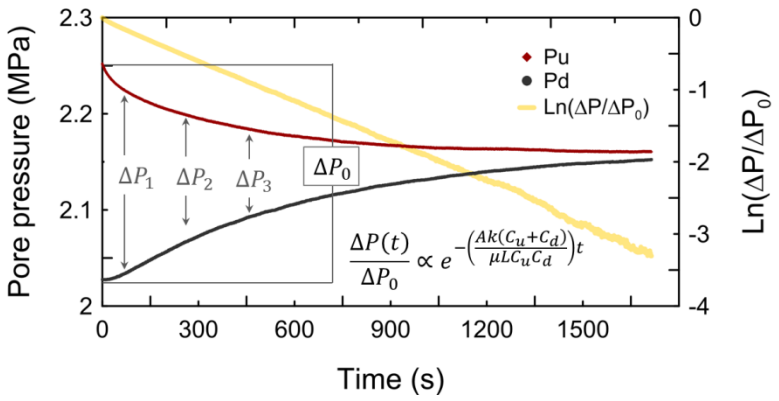

Figure 8. Example of application of the pulse decay method (PDM) over a granite sample confined at 25 MPa. The evolution of pore pressure evolution at the upstream (P_u) and downstream (P_d) ends are also illustrated.

1.3 Pore Pressure Transmission Method (PPTM)

The PPTM method differs from the PDM by the fact that the upstream reservoir is kept at a constant pressure while in the downstream reservoir pressure starts at a significantly lower value. This reservoir is initially isolated so that the pressure recording starts once the valve connecting the downstream reservoir and the sample becomes open. Obviously, there is no pressure evolution in the upstream reservoir (*i.e.* it shows a constant value). However, the pressure in the downstream reservoir rises exponentially. The mathematical expression theoretically describing this evolution is presented in equation e.4 (Metwally and Sondergeld, 2011):

$$\partial P(t) = f_1 exp\left(\frac{-\theta^2 k}{\mu L^2 B_f \phi_e}\right) \qquad \text{e.4}$$

where f_1 is a lumped parameter integrating the fluid storage capacities of the up- and downstream reservoirs which also depends on the initial pressure gradient imposed on the system. However, because the test is aimed at determining permeability (whose value only appears equated in the exponential part of the expression e.4) it is convenient to linearize it by considering the natural logarithm of the differential pressure and plotting it against time. Therefore, permeability can be directly linked to the experimental slope, α, according with:

$$k = \frac{\alpha \mu L^2 B_f \phi_e}{-\theta^2} \qquad \text{e.5}$$

in which B_f is the static compressibility of the fluid (Pa^{-1}) and ϕ_e the effective porosity of the sample. The term θ lumps together the volumes of the up- and downstream reservoirs and the pore space of the sample (V_p):

$$tan\theta = \frac{(\varphi + \gamma)\theta}{\theta^2 - \varphi\gamma} \qquad \text{e.6}$$

being $\varphi = V_p/V_u$ and $\gamma = V_p/V_d$. Considering an infinite upstream reservoir volume (*i.e.* $\varphi = 0$) then $tan\theta = \gamma/\theta$.

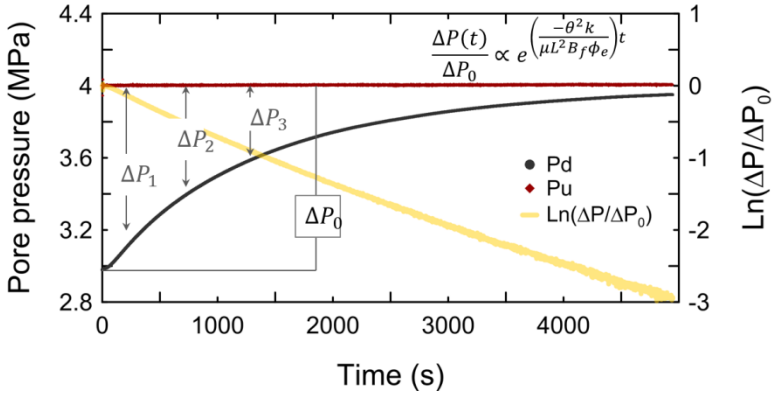

Figure 9. Example of application of the pore pressure transmission method (PPTM) on a granite sample confined at 15 MPa. The evolution of pore pressure evolution at the upstream (P_u) and downstream (P_d) ends are also illustrated.

According to Metwally and Sondergeld (2011), when using a liquid as permeating fluid, the compressibility of the reservoirs can be determined before testing any sample from equation e.7 according to the following procedure: Firstly, insert a solid stainless steel cylinder into the cell (*i.e.* porosity=0; permeability=0); Secondly, calculate the liquid compressibility β_l from the syringe pump volume V_0, imposing a ΔP sequence and measuring the associated ΔV; Thirdly, once knowing β_l, the volume of each reservoir results from applying the above procedure to create their own $\Delta V/\Delta P$ coefficients.

$$\beta_l = \frac{\Delta V/\Delta P}{V_0} \qquad \text{e.7}$$

Furthermore, equation e.7 highlights why the pulse decay method approximates the permeability from the compressive storage coefficients of up- and downstream reservoirs instead of their respective volumes (*i.e.*, assuming β_l constant for a given hydraulically closed circuit).

The calibration of system compressibility coefficients and reservoir volumes appears to be a critical factor when considering the application of the PDT and PPTM techniques. It is worth noting, however, that the SSFM can be used to better constrain these parameters, in particular if we set up our experimental system considering a pressure gradient equal to that envisaged for the PPTM (for instance 2 to 3 MPa, from up- to downstream). Therefore, with a back calculation procedure, using the

permeability value carefully obtained with the SSFM method, we can better evaluate (or corroborate) the upstream and downstream volumes as well as the corresponding system's compressibility coefficients.

4. Case Study

All three SSFM, PDM and PPTM have been applied to two granite samples under different confining and pore pressures. The tested specimens (Figure 10) were cylindrical, with 86.4 and 74.52 mm length and 38.74 and 53.52 mm diameter, respectively. In each case, porosity was close to 1 and 1.2 %, respectively. The plugs were mounted into a Hassler and a modified Hoek-Franklin cells located inside a thermal isolation chamber. Permeability was measured repeatedly under varying isotropic ($\sigma_1=\sigma_2=\sigma_3$) and non-isotropic ($\sigma_1\neq\sigma_2=\sigma_3$) confining stresses and differential pressure conditions.

Figure 10 shows a summary of the results obtained in the tests and appendix III display an extensive graphical summary of the experimental results. The PDM and PPTM transient methods were performed under a hydrostatic pressure of 15, 20 and 25 MPa while for the SSFM, in addition to the previous 30 MPa of confining conditions was also tested.

Overall, the experimental results obtained with the three methods are consistent and we can observe a relatively small dispersion in the values (which is more apparent in figure 10 due to the scale of representation). However, it is worth mentioning that the permeability *vs.* confining pressure distribution experimentally obtained differs to what intuitively should be expected: That is, a reduction in permeability when confining pressure rises due to the progressive reduction porosity. In Figure 10 we observe that, although this tendency is apparent from 15 to 25 and 30 MPa, the results at 20 MPa are higher than at 15 MPa. This inconsistency can be explained by considering the presence of compliant pores and its orientation with respect to the imposed stress field. In this context, it is interesting to observe Figure 11, where a similar granite plug (but with larger size) was submitted to a non-isotropic stress field during the execution of PDM tests. We observe that permeability increases as the axial stress rises what suggests the progressive opening of compliant pores whose orientation would be roughly parallel to σ_1.

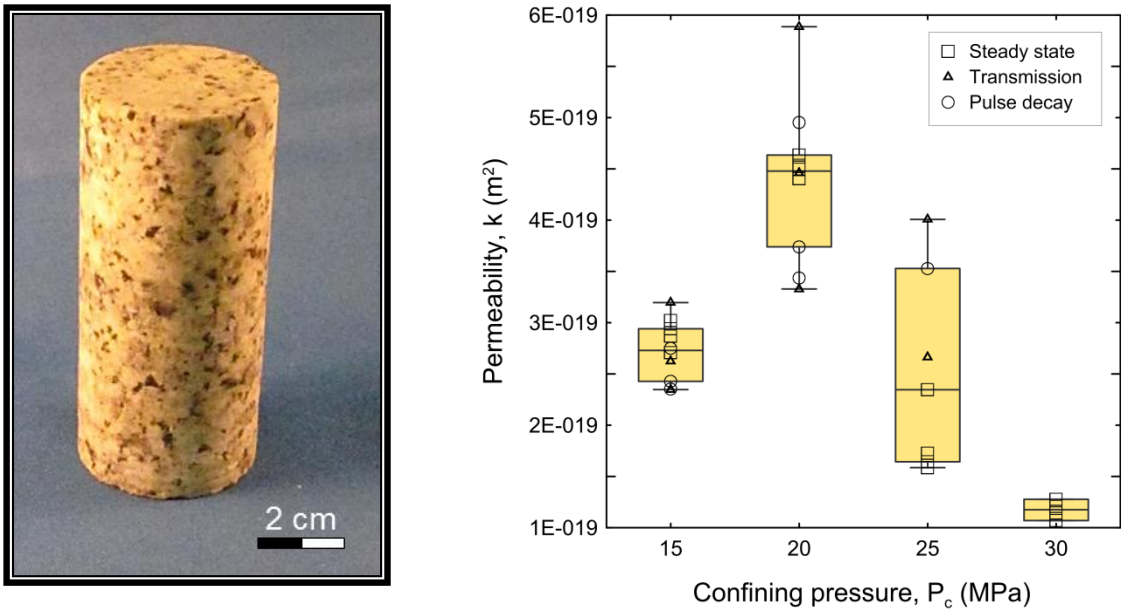

Figure 10. ***Left*****.** Granite tested plug, using the Hassler cell. ***Right*****.** Results of the permeability determinations performed at 30 MPa confining pressure using the three described experimental methods. The box and whisper (yellow) diagram illustrates permeability distribution for each step of confining pressure, considering the three methods.

In the same Figure 11, we can also compare results obtained using the two described core-holders for equivalent experimental conditions. We observe a good correspondence of permeability values what suggests that both the Hassler and the Hoek-Franklin cells perform equally well in the experiments developed.

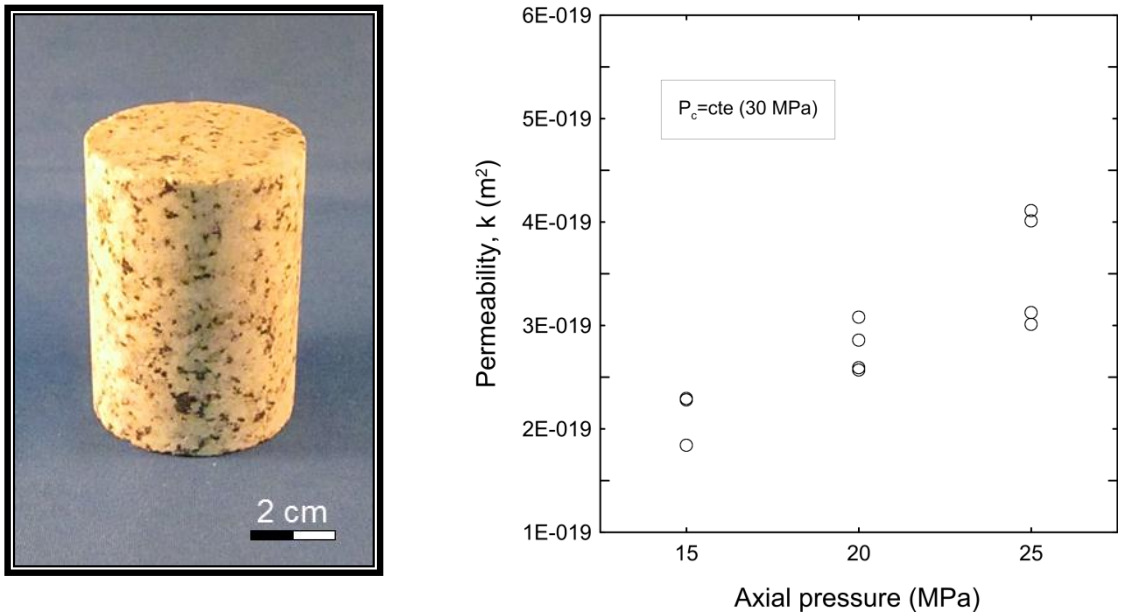

Figure 11. ***Left*****.** Granite tested plug using the Hoek-Franklin cell. ***Right.*** Permeability determinations performed with the granite sample using the PDM method under constant confining pressure (σ_2=σ_3=30 MPa) and variable axial stress (σ_1=15, 20, 25 MPa).

5. References

Boulin, P.F., Bretonnier, P., Gland, N. and Lombard, J.M. (2012) Contribution of the steady state method to water permeability measurement in very low permeability porous media. Oil Gas Sci. Tech. – IFP Energies Nouvelles 1-15. (doi:10.2516/ogst/2011169)

Bourlange, S., Jouniaux, L. and Henry, P. (2004) Data report: Permeability, compressibility, and friction coefficient measurements under confining pressure and strain, Leg 190, Nankai Trough. *In*: H. Mikada, Moore, G.F., Taira, A., Becker, K., Moore, J.C., and Klaus, A. (Eds.), Proceedings of the Ocean Drilling Project Scientific Results Vol. 190/196, 1-16

Brace, W.F., Walsh, J.B. and Frangos, W.T. (1968) Permeability of granite under high pressure. J. Geophys. Res. 73(6), 2225-2236

Cui, X., Bustin, A.M.M. and Bustin, R.M. (2009) Measurements of gas permeability and diffusivity of tight reservoir rocks: Different approaches and their applications. Geofluids 9, 208-223 (doi:10.1111/j.1468-8123.2009.00244.x)

Cui, X., Bustin, R.M., Brezovski, R., Nassichuk, B., Glover, G and Pathi, V.S. (2010) A new method to simultaneously measure in-situ permeability and porosity under reservoir conditions: implications for characterization of unconventional gas. Canadian Unconventional Resources and International Petroleum Conference, 19-21 October 2010, Calgary, Alberta, Canada. SPE 138148 (doi: 10.2118/138148-MS)

Hassler, G. L. (1944) Method and apparatus for permeability measurements. U. S. Patent No. 2345935

Hoek, E. and Franklin, J.A. (1968) Simple triaxial cell for field or laboratory testing of rock. Transactions of the Institute of Mining and Metallurgy 77, 22-26

Hoff, W.D. and Hall, C. (2002) Water transport in brick, stone and concrete. Taylor & Francis, 318 p.

Jouniaux, L., Lallemant, S., Pozzi, J. and Pierre (1994) Changes in the permeability, streaming potential and resistivity of a claystone from the Nankai prism under stress. Geophys. Res. Let. 21, 149-152

Metwally, Y.M. and Sondergeld, C.H. (2011) Measuring low permeabilities of gas-sands and shales using a pressure transmission technique. Int. J. Rock Mech. Min. Sci. 48, 1135-1144 (doi: 10.1016/j.ijrmms.2011.08.004)

Reuschle, T. (2011) Data report: permeability measurements under confining pressure, Expeditions 315 and 316, Nankai Trough. *In*: M. Kinoshita, Tobin, H., Ashi, J., Kimura, G., Lallemant, S., Screaton, E.J., Curewitz, D., Masago, H., Moe, K.T., and the Expedition 314/315/316 Scientists (Eds.), Proceedings of the Integrated Ocean Drilling Program, Vol. 314/315/316, 1-17 (doi:10.2204/iodp.proc.314315316.205.2011)

Appendix I. Utilities for Data Reduction and Processing

Due to the great amount of information produced during the development of each experiment, it is important to have an adequate strategy of data reduction and data analysis. In our case we have developed a number of Excel® utilities useful to deal with large amount of numerical records. These utilities are based on dynamic tables allowing the easy zooming and segmentation of a selected data range.

When opening any of the three utility tables, one must fill out the key cells depending on the test performed (*i.e.* SSFM, PDM, PPTM methods, respectively) with the experimental data, as it is shown in Figures 12, 13, 14 and 15. The three tables include a common set of parameters concerning the rock sample, fluid properties and experimental conditions. In the case of the PDM and PPTM methods, the compressibility storage coefficients, water compressibility and porosity constitute critical data to compute permeability. Permeability is automatically evaluated from the experimental data range selected.

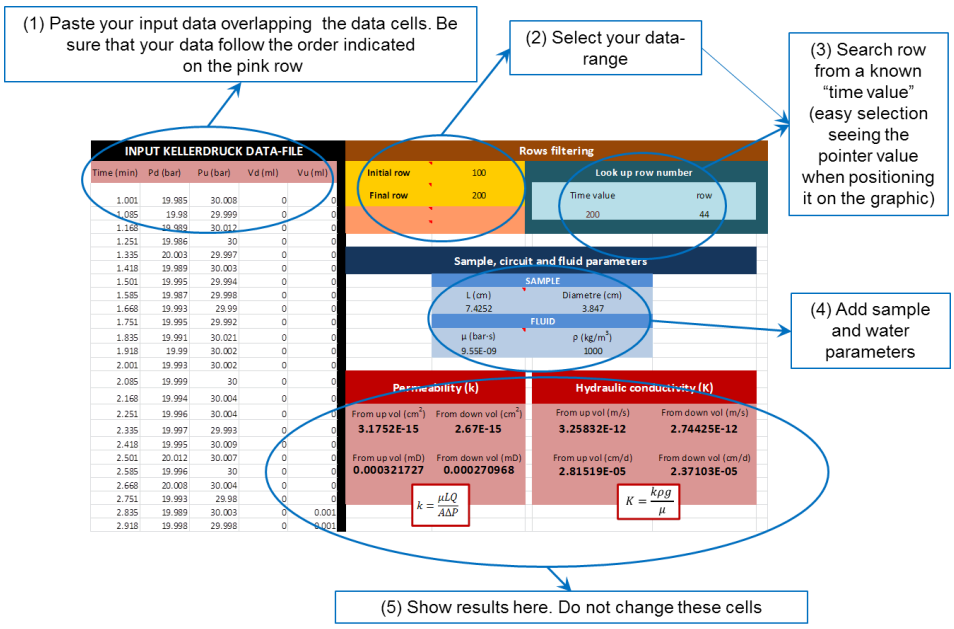

Figure 12. Example of dynamic table used to calculate permeabilities from SSFM method.

When applying the pulse decay method, temperature fluctuations play an important role. The dynamic table integrates a numerical slope decay corrector that can be fixed by the user: *Slope (ini-row)* to *Slope (fin-row)*. That means that the user is free to decide when he considers that the up- and downstream pressures have equilibrated defining a data range representative of the observed decay from hereafter (*i.e.* the same decay effect due to the temperature fluctuation occurs at any

time of the test but it is easier appreciated at the end). Figures 16-32 show examples of such an effect and the correction performed with the dynamic table.

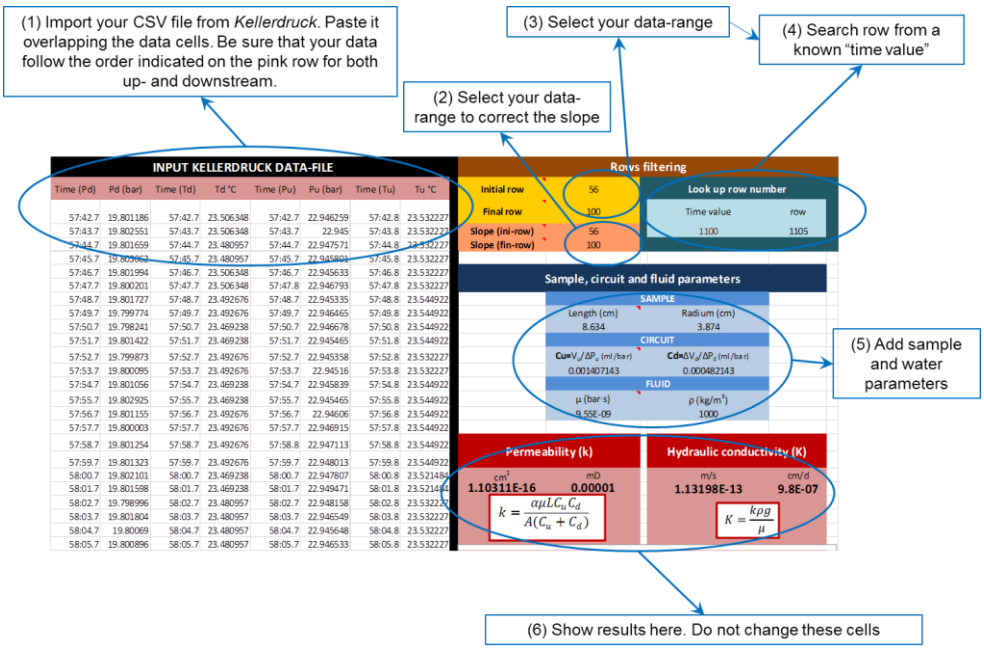

Figure 13. Example dynamic table to calculate permeabilities from the PDM.

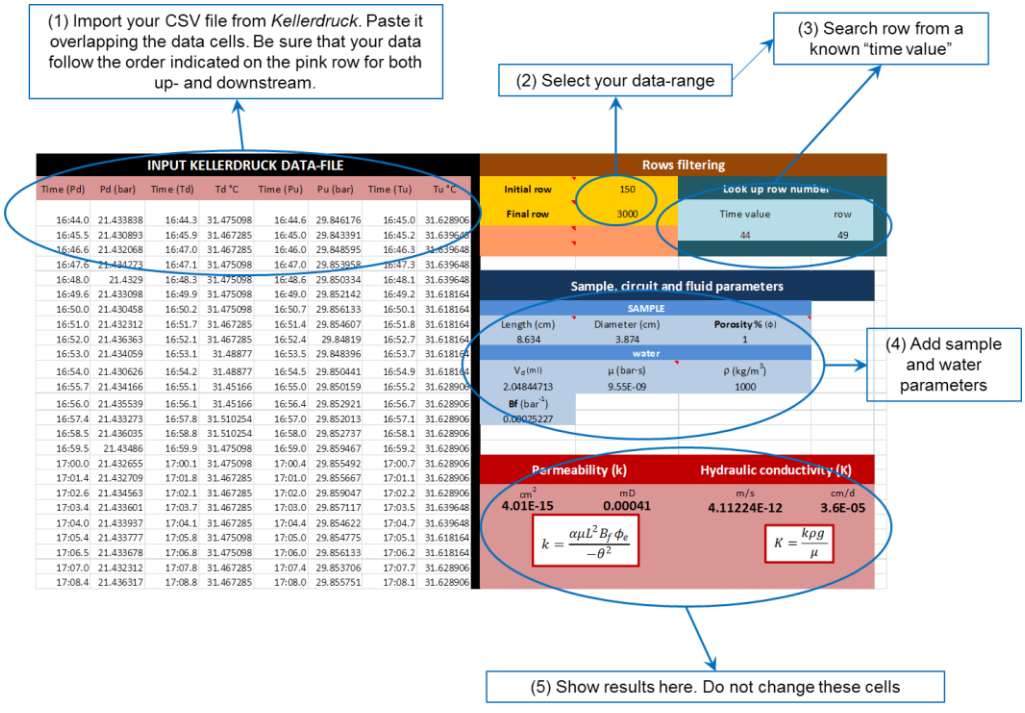

Figure 14. Dynamic table to calculate permeabilities from the pore pressure transmision method, filling out cells in the format imported from *Kellerdruck software*®.

Appendix II. Quizix Batch Command Sequence Example

The Quizix system allows the user to automate the work where possible. In this section, we present two useful batch-command sequences. Taking it as a template, it is relatively simple to adapt it for more complex operations.

1.1 Batch Command Sequence for the Calibration of Fluid Reservoirs

```
#This sequence allow the user obtain the compressibility coefficients of reservoirs
#Set data-logging at 1s.
1,0,=,0,2,|,0,>,0,2,DATALOG,0.017,0,>,0,2,&,0,>,0,2,NULL,0,0,NULL,0
#Set pumps on
20,0,=,0,2,|,0,=,0,2,1:SET_CYL1_ON,1,0,>,0,2,&,0,>,0,2,NULL,0,0,NULL,0
30,0,=,0,2,|,0,=,0,2,2:SET_CYL2_ON,1,0,>,0,2,&,0,>,0,2,NULL,0,0,NULL,0
#Ramp up 80 bar (5min)
40,0,=,0,2,&,0,=,0,2,1:RAMP,1;ON;2;5;80,0,>,0,2,&,0,>,0,2,NULL,0,0,NULL,0
50,0,=,0,2,&,0,=,0,2,2:RAMP,1;ON;2;5;80,0,>,0,2,&,0,>,0,2,NULL,0,0,NULL,0
#Hold pressures during 10 min
53,0,=,0,720,|,0,>,0,2,NULL,0,0,>,0,2,&,0,>,0,2,NULL,0,0,NULL,0
#Ramp up 1 bar (5min)
60,0,=,0,2,&,0,=,0,2,1:RAMP,1;ON;2;5;1,0,>,0,2,&,0,>,0,2,NULL,0,0,NULL,0
70,0,=,0,2,&,0,=,0,2,2:RAMP,1;ON;2;5;1,0,>,0,2,&,0,>,0,2,NULL,0,0,NULL,0
#Hold pressures during 10 min
80,0,=,0,720,|,0,>,0,2,NULL,0,0,>,0,2,&,0,>,0,2,NULL,0,0,NULL,0
#Ramp up 1.5 bar (2min)
90,0,=,0,2,&,0,=,0,2,1:RAMP,1;ON;2;2;1.5,0,>,0,2,&,0,>,0,2,NULL,0,0,NULL,0
95,0,=,0,2,&,0,=,0,2,2:RAMP,1;ON;2;2;1.5,0,>,0,2,&,0,>,0,2,NULL,0,0,NULL,0
# Hold pressures during 10 min
98,0,=,0,720,|,0,>,0,2,NULL,0,0,>,0,2,&,0,>,0,2,NULL,0,0,NULL,0
#Ramp up 2.5 bar (2min)
100,0,=,0,2,&,0,=,0,2,1:RAMP,1;ON;2;2;2.5,0,>,0,2,&,0,>,0,2,NULL,0,0,NULL,0
150,0,=,0,2,&,0,=,0,2,2:RAMP,1;ON;2;2;2.5,0,>,0,2,&,0,>,0,2,NULL,0,0,NULL,0
#Hold pressures during 10 min
153,0,=,0,720,|,0,>,0,2,NULL,0,0,>,0,2,&,0,>,0,2,NULL,0,0,NULL,0
#Ramp up 5 bar (2min)
160,0,=,0,2,&,0,=,0,2,1:RAMP,1;ON;2;2;5,0,>,0,2,&,0,>,0,2,NULL,0,0,NULL,0
170,0,=,0,2,&,0,=,0,2,2:RAMP,1;ON;2;2;5,0,>,0,2,&,0,>,0,2,NULL,0,0,NULL,0
#Hold pressures during 10 min
173,0,=,0,720,|,0,>,0,2,NULL,0,0,>,0,2,&,0,>,0,2,NULL,0,0,NULL,0
#Ramp up 10 bar (2min)
180,0,=,0,2,&,0,=,0,2,1:RAMP,1;ON;2;2;10,0,>,0,2,&,0,>,0,2,NULL,0,0,NULL,0
190,0,=,0,2,&,0,=,0,2,2:RAMP,1;ON;2;2;10,0,>,0,2,&,0,>,0,2,NULL,0,0,NULL,0
#Hold pressures during 10 min
193,0,=,0,720,|,0,>,0,2,NULL,0,0,>,0,2,&,0,>,0,2,NULL,0,0,NULL,0
#Ramp up15 bar (2min)
200,0,=,0,2,&,0,=,0,2,1:RAMP,1;ON;2;2;15,0,>,0,2,&,0,>,0,2,NULL,0,0,NULL,0
250,0,=,0,2,&,0,=,0,2,2:RAMP,1;ON;2;2;15,0,>,0,2,&,0,>,0,2,NULL,0,0,NULL,0
#Hold pressures during 10 min
253,0,=,0,720,|,0,>,0,2,NULL,0,0,>,0,2,&,0,>,0,2,NULL,0,0,NULL,0
#Ramp up20 bar (2min)
260,0,=,0,2,&,0,=,0,2,1:RAMP,1;ON;2;2;20,0,>,0,2,&,0,>,0,2,NULL,0,0,NULL,0
270,0,=,0,2,&,0,=,0,2,2:RAMP,1;ON;2;2;20,0,>,0,2,&,0,>,0,2,NULL,0,0,NULL,0
#Hold pressures during 10 min
273,0,=,0,720,|,0,>,0,2,NULL,0,0,>,0,2,&,0,>,0,2,NULL,0,0,NULL,0
#Ramp up30 bar (2min)
280,0,=,0,2,&,0,=,0,2,1:RAMP,1;ON;2;2;30,0,>,0,2,&,0,>,0,2,NULL,0,0,NULL,0
290,0,=,0,2,&,0,=,0,2,2:RAMP,1;ON;2;2;30,0,>,0,2,&,0,>,0,2,NULL,0,0,NULL,0
#Hold pressures during 10 min
300,0,=,0,720,|,0,>,0,2,NULL,0,0,>,0,2,&,0,>,0,2,NULL,0,0,NULL,0
#Ramp up40 bar (2min)
310,0,=,0,2,&,0,=,0,2,1:RAMP,1;ON;2;2;40,0,>,0,2,&,0,>,0,2,NULL,0,0,NULL,0
320,0,=,0,2,&,0,=,0,2,2:RAMP,1;ON;2;2;40,0,>,0,2,&,0,>,0,2,NULL,0,0,NULL,0
#Hold pressures during 10 min
323,0,=,0,720,|,0,>,0,2,NULL,0,0,>,0,2,&,0,>,0,2,NULL,0,0,NULL,0
```

```
#Ramp up50 bar (2min)
330,0,=,0,2,&,0,=,0,2,1:RAMP,1;ON;2;2;50,0,>,0,2,&,0,>,0,2,NULL,0,0,NULL,0
340,0,=,0,2,&,0,=,0,2,2:RAMP,1;ON;2;2;50,0,>,0,2,&,0,>,0,2,NULL,0,0,NULL,0
#Hold pressures during 10 min
343,0,=,0,720,|,0,>,0,2,NULL,0,0,>,0,2,&,0,>,0,2,NULL,0,0,NULL,0
#Ramp up60 bar (2min)
350,0,=,0,2,&,0,=,0,2,1:RAMP,1;ON;2;2;60,0,>,0,2,&,0,>,0,2,NULL,0,0,NULL,0
355,0,=,0,2,&,0,=,0,2,2:RAMP,1;ON;2;2;60,0,>,0,2,&,0,>,0,2,NULL,0,0,NULL,0
#Hold pressures during 10 min
360,0,=,0,720,|,0,>,0,2,NULL,0,0,>,0,2,&,0,>,0,2,NULL,0,0,NULL,0
#Ramp up70 bar (2min)
370,0,=,0,2,&,0,=,0,2,1:RAMP,1;ON;2;2;70,0,>,0,2,&,0,>,0,2,NULL,0,0,NULL,0
380,0,=,0,2,&,0,=,0,2,2:RAMP,1;ON;2;2;70,0,>,0,2,&,0,>,0,2,NULL,0,0,NULL,0
#Hold pressures during 10 min
390,0,=,0,720,|,0,>,0,2,NULL,0,0,>,0,2,&,0,>,0,2,NULL,0,0,NULL,0
#Ramp up80 bar (2min)
400,0,=,0,2,&,0,=,0,2,1:RAMP,1;ON;2;2;80,0,>,0,2,&,0,>,0,2,NULL,0,0,NULL,0
410,0,=,0,2,&,0,=,0,2,2:RAMP,1;ON;2;2;80,0,>,0,2,&,0,>,0,2,NULL,0,0,NULL,0
#Hold pressures during 10 min
413,0,=,0,720,|,0,>,0,2,NULL,0,0,>,0,2,&,0,>,0,2,NULL,0,0,NULL,0
#Ramp up1 bar (5min)
660,0,=,0,2,&,0,=,0,2,1:RAMP,1;ON;2;5;1,0,>,0,2,&,0,>,0,2,NULL,0,0,NULL,0
670,0,=,0,2,&,0,=,0,2,2:RAMP,1;ON;2;5;1,0,>,0,2,&,0,>,0,2,NULL,0,0,NULL,0
#Hold 5 min
680,0,=,0,300,|,0,>,0,2,NULL,0,0,>,0,2,&,0,>,0,2,NULL,0,0,NULL,0
685,0,=,0,2,|,0,=,0,2,1:SET_CYL1_OFF,0,0,>,0,2,&,0,>,0,2,NULL,0,0,NULL,0
686,0,=,0,2,|,0,=,0,2,2:SET_CYL2_OFF,0,0,>,0,2,&,0,>,0,2,NULL,0,0,NULL,0
#Set data-logging a 120 min
700,0,=,0,2,|,0,>,0,2,DATALOG,120,0,>,0,2,&,0,>,0,2,NULL,0,0,NULL,0
```

1.2 Batch Command Sequence for Applying the Steady State Flow Method

```
#This sequence allow the user to automatically obtain the permeability from the steady
#state method at different pressure gradients.
#Test beginning. Set data-logging at 10s.
1,0,=,0,2,|,0,>,0,2,DATALOG,0.17,0,>,0,2,&,0,>,0,2,NULL,0,0,NULL,0
20,0,=,0,2,|,0,=,0,2,1:SET_CYL1_ON,1,0,>,0,2,&,0,>,0,2,NULL,0,0,NULL,0
30,0,=,0,2,|,0,=,0,2,2:SET_CYL2_ON,1,0,>,0,2,&,0,>,0,2,NULL,0,0,NULL,0
#Ramp up 30 bar Upstream and 20 bar downstream (5min)
40,0,=,0,2,&,0,=,0,2,1:RAMP,1;ON;2;5;20,0,>,0,2,&,0,>,0,2,NULL,0,0,NULL,0
50,0,=,0,2,&,0,=,0,2,2:RAMP,1;ON;2;5;30,0,>,0,2,&,0,>,0,2,NULL,0,0,NULL,0
51,CV11,!=,0,2,|,CV12,!=,0,2,1:RESET_ALL,0,CV21,!=,0,2,|,CV22,!=,0,2,1:RESET_ALL,0,0,NUL
L,0
52,CV21,!=,0,2,|,CV22,!=,0,2,2:RESET_ALL,0,0,>,0,2,&,0,>,0,2,1:RESET_ALL,0,0,NULL,0
#Hold current pressures during 5 hours
53,0,=,0,18000,|,0,>,0,2,NULL,0,0,>,0,2,&,0,>,0,2,NULL,0,0,NULL,0
# Ramp up 40 bar Upstream and 25 bar downstream (5min)
60,0,=,0,2,&,0,=,0,2,1:RAMP,1;ON;2;5;25,0,>,0,2,&,0,>,0,2,NULL,0,0,NULL,0
70,0,=,0,2,&,0,=,0,2,2:RAMP,1;ON;2;5;40,0,>,0,2,&,0,>,0,2,NULL,0,0,NULL,0
#Hold current pressures during 5 hours
73,0,=,0,18000,|,0,>,0,2,NULL,0,0,>,0,2,&,0,>,0,2,NULL,0,0,NULL,0
# Ramp up 50 bar Upstream and 20 bar downstream (5min)
80,0,=,0,2,&,0,=,0,2,1:RAMP,1;ON;2;5;20,0,>,0,2,&,0,>,0,2,NULL,0,0,NULL,0
81,0,=,0,2,&,0,=,0,2,2:RAMP,1;ON;2;5;50,0,>,0,2,&,0,>,0,2,NULL,0,0,NULL,0
#Hold current pressures during 5 hours
83,0,=,0,18000,|,0,>,0,2,NULL,0,0,>,0,2,&,0,>,0,2,NULL,0,0,NULL,0
# Ramp up 60 bar Upstream and 20 bar downstream (5min)
90,0,=,0,2,&,0,=,0,2,1:RAMP,1;ON;2;5;20,0,>,0,2,&,0,>,0,2,NULL,0,0,NULL,0
91,0,=,0,2,&,0,=,0,2,2:RAMP,1;ON;2;5;60,0,>,0,2,&,0,>,0,2,NULL,0,0,NULL,0
#Hold current pressures during 5 hours
93,0,=,0,18000,|,0,>,0,2,NULL,0,0,>,0,2,&,0,>,0,2,NULL,0,0,NULL,0
#Switch off
685,0,=,0,2,|,0,=,0,2,1:SET_CYL1_OFF,0,0,>,0,2,&,0,>,0,2,NULL,0,0,NULL,0
686,0,=,0,2,|,0,=,0,2,2:SET_CYL2_OFF,0,0,>,0,2,&,0,>,0,2,NULL,0,0,NULL,0
#Set data-logging at 30 min
700,0,=,0,2,|,0,>,0,2,DATALOG,30,0,>,0,2,&,0,>,0,2,NULL,0,0,NULL,0
```

Appendix III. Graphical Display of Experimental Results

1.1 Steady State Method

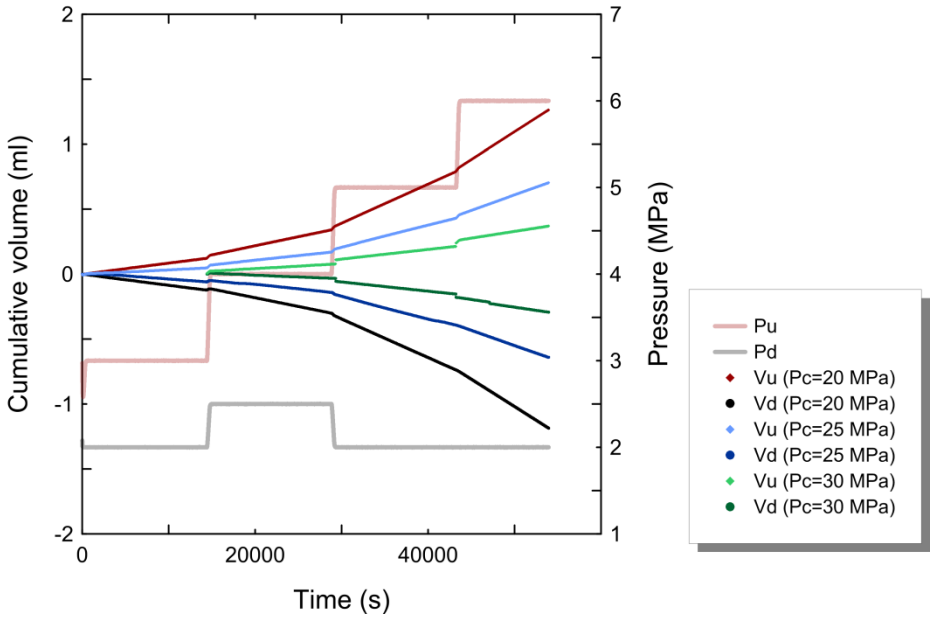

Figure 15. Results of the SSFM method tests on a granite sample submitted to different hydrostatic pressures and different pressure gradients (i.e., difference between up- and downstream pressures: Pu – Pd). Vu and Vd represent water volumes at the inlet and outlet, respectively.

1.2 Pulse Decay Method

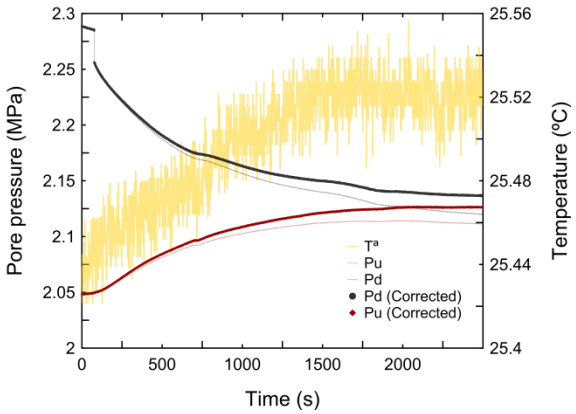

Figure 16. PDM on a granite sample confined at hydrostatic pressure of 15 MPa. Initial upstream and incremental pressures of Pu~2.25 MPa and ΔP_0~0.2 MPa. Temperature evolution is also illustrated.

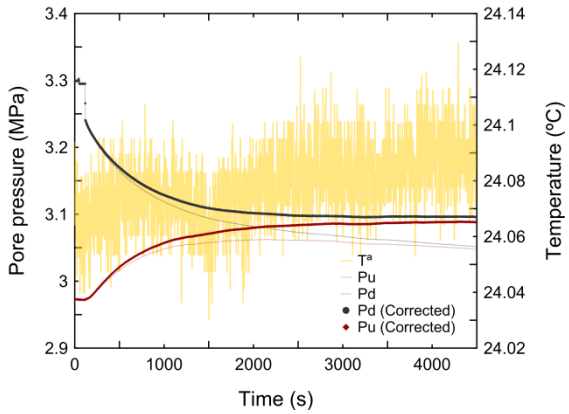

Figure 17. PDM on a granite sample confined at hydrostatic pressure of 15 MPa. Initial upstream and incremental pressures of Pu~3.24 MPa and ΔP_0~0.3 MPa. Temperature evolution is also illustrated.

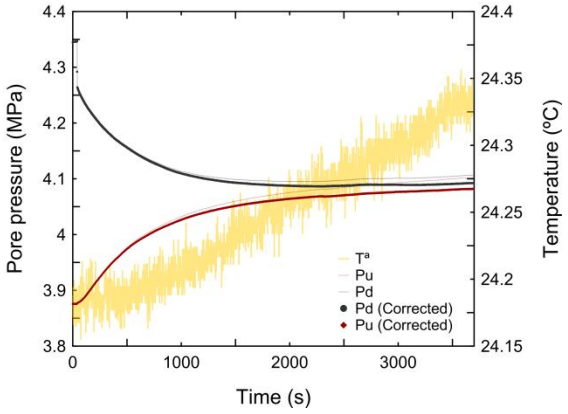

Figure 18. PDM on a granite sample confined at hydrostatic pressure of 15 MPa. Initial upstream and incremental pressures of Pu~4.27 MPa and ΔP_0~0.4 MPa. Temperature evolution is also illustrated.

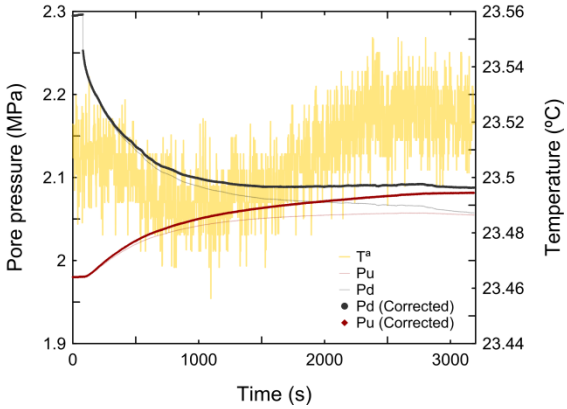

Figure 19. PDM on a granite sample confined at hydrostatic pressure of 20 MPa. Initial upstream and incremental pressures of Pu~2.26 MPa and ΔP_0~0.28 MPa. Temperature evolution is also illustrated.

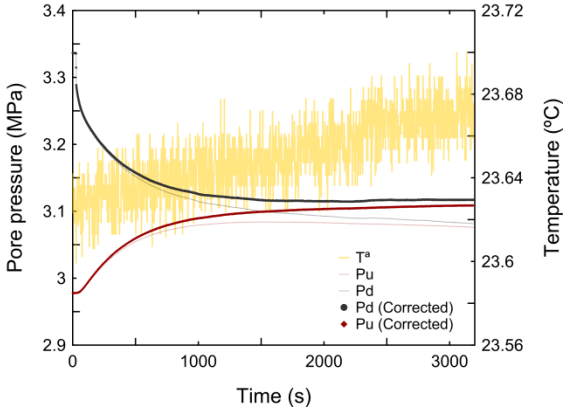

Figure 20. PDM on a granite sample confined at hydrostatic pressure of 20 MPa. Initial upstream and incremental pressures of Pu~3.28 MPa and ΔP_0~0.3 MPa. Temperature evolution is also illustrated.

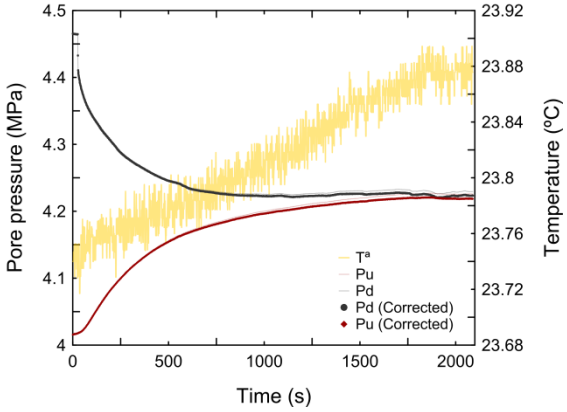

Figure 21. PDM on a granite sample confined at hydrostatic pressure of 20 MPa. Initial upstream and incremental pressures of Pu~4.42 MPa and ΔP_0~0.4 MPa. Temperature evolution is also illustrated.

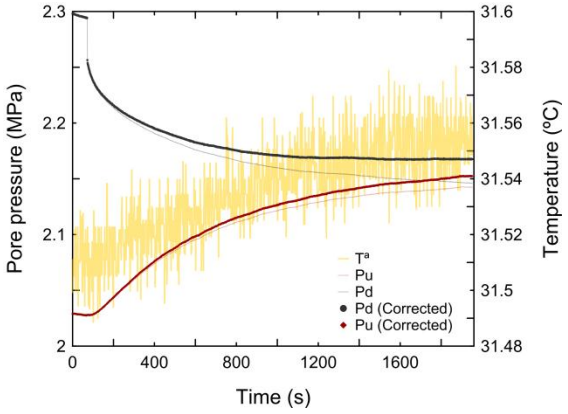

Figure 22. PDM on a granite sample confined at hydrostatic pressure of 25 MPa. Initial upstream and incremental pressures of Pu~2.26 MPa and ΔP_0~0.23 MPa. Temperature evolution is also illustrated.

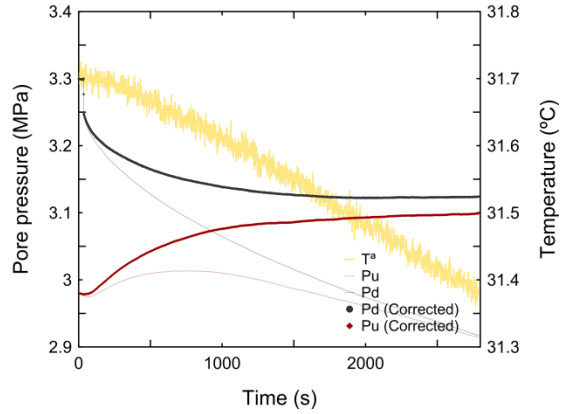

Figure 23. PDM on a granite sample confined at hydrostatic pressure of 25 MPa. Initial upstream and incremental pressures of Pu~3.26 MPa and ΔP_0~0.3 MPa. Temperature evolution is also illustrated.

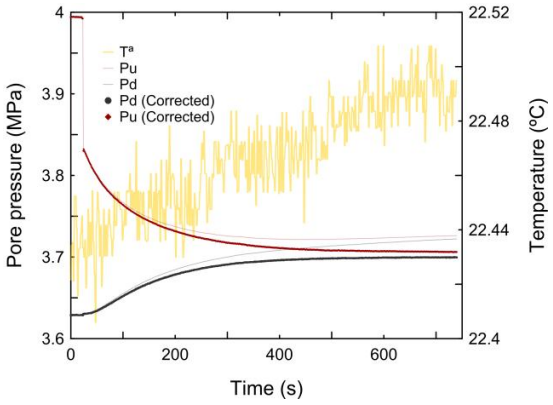

Figure 24. PDM on a granite sample at 30 MPa of confining pressure and 15 MPa of axial stress. Initial upstream and incremental pressures of Pu~3.84 MPa and ΔP_0~0.2 MPa. Temperature evolution is also illustrated.

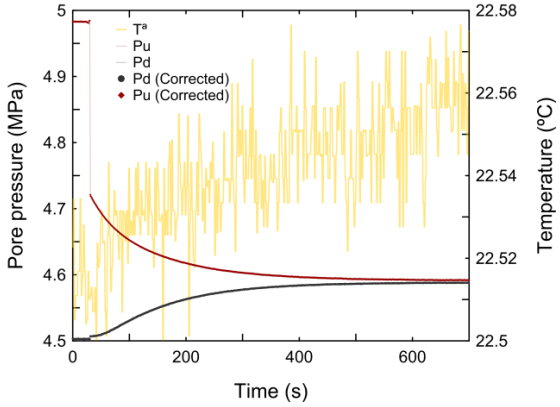

Figure 25. PDM on a granite sample at 30 MPa of confining pressure and 15 MPa of axial stress. Initial upstream and incremental pressures of Pu~4.84 MPa and ΔP_0~0.22 MPa. Temperature evolution is also illustrated.

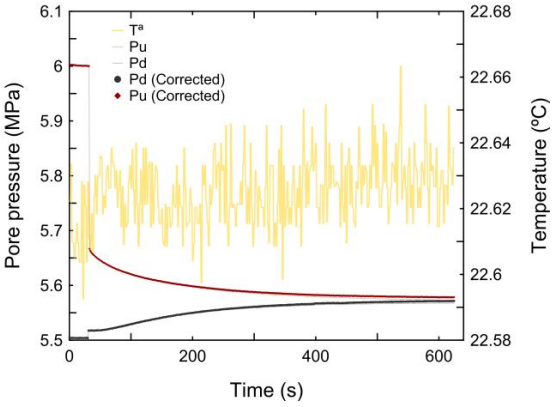

Figure 26. PDM on a granite sample at 30 MPa of confining pressure and 15 MPa of axial stress. Initial upstream and incremental pressures of Pu~5.67 MPa and ΔP_0~0.16 MPa. Temperature evolution is also illustrated.

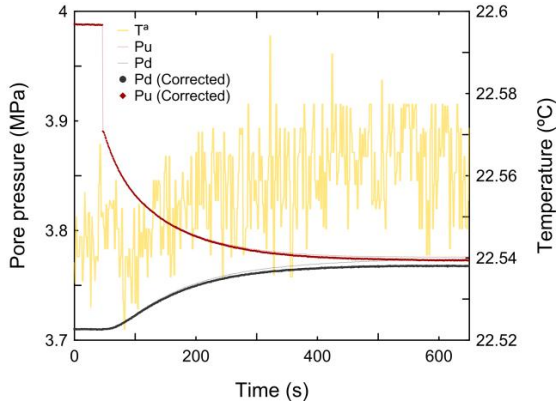

Figure 27. PDM on a granite sample at 30 MPa of confining pressure and 20 MPa of axial stress. Initial upstream and incremental pressures of Pu~3.89 MPa and ΔP_0~0.18 MPa. Temperature evolution is also illustrated.

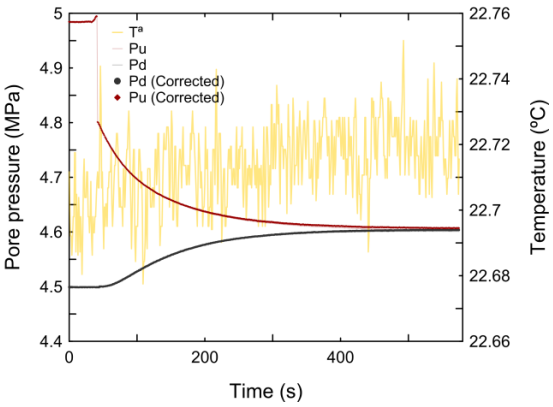

Figure 28. PDM on a granite sample at 30 MPa of confining pressure and 20 MPa of axial stress. Initial upstream and incremental pressures of Pu~4.8 MPa and ΔP_0~0.3 MPa. Temperature evolution is also illustrated.

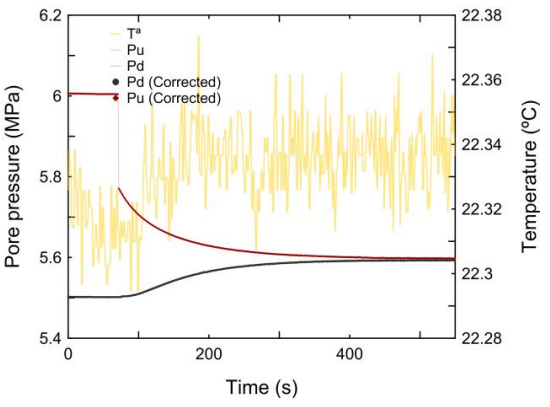

Figure 29. PDM on a granite sample at 30 MPa of confining pressure and 20 MPa of axial stress. Initial upstream and incremental pressures of Pu~5.78 MPa and ΔP_0~0.3 MPa. Temperature evolution is also illustrated.

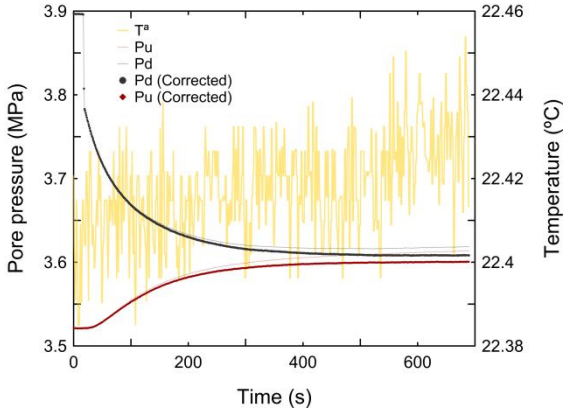

Figure 30. PDM on a granite sample at 30 MPa of confining pressure and 25 MPa of axial stress. Initial upstream and incremental pressures of Pu~3.78 MPa and ΔP_0~0.25 MPa. Temperature evolution is also illustrated.

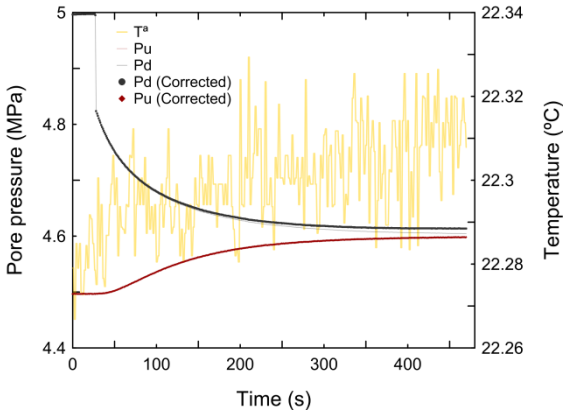

Figure 31. PDM on a granite sample at 30 MPa of confining pressure and 25 MPa of axial stress. Initial upstream and incremental pressures of Pu~4.82 MPa and ΔP_0~0.32 MPa. Temperature evolution is also illustrated.

1.3 Pore Pressure Transmision Method

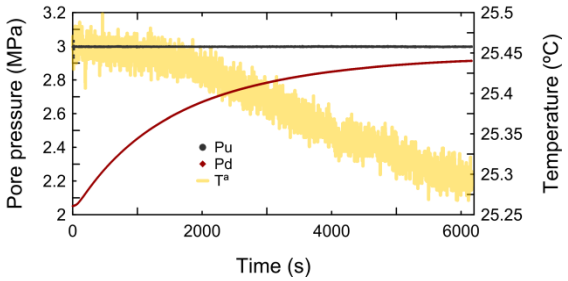

Figure 32. PPTM on a granite sample confined at hydrostatic pressure of 15 MPa. Initial upstream and incremental pressures of Pu~3 MPa and ΔP_0~1 MPa. Temperature evolution is also illustrated.

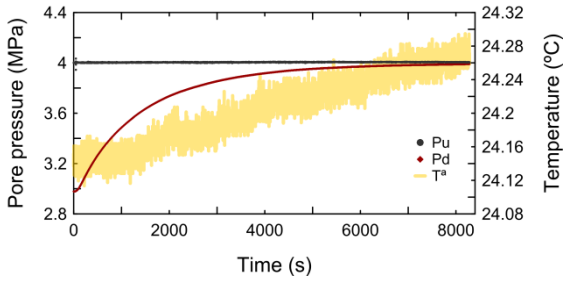

Figure 33. PPTM on a granite sample confined at hydrostatic pressure of 15 MPa. Initial upstream and incremental pressures of Pu~4 MPa and ΔP_0~1 MPa. Temperature evolution is also illustrated.

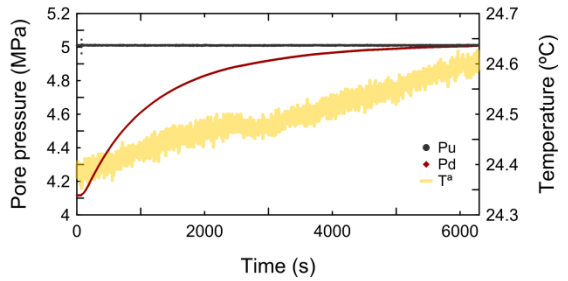

Figure 34. PPTM on a granite sample confined at hydrostatic pressure of 15 MPa. Initial upstream and incremental pressures of Pu~5 MPa and ΔP_0~0.9 MPa. Temperature evolution is also illustrated.

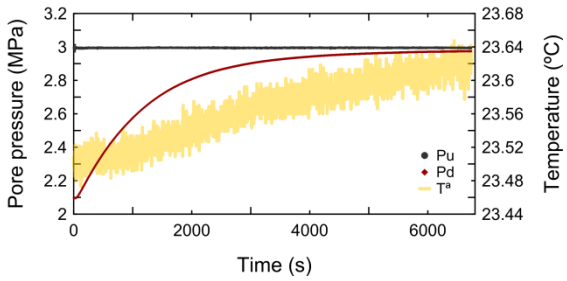

Figure 35. PPTM on a granite sample confined at hydrostatic pressure of 20 MPa. Initial upstream and incremental pressures of Pu~3 MPa and ΔP_0~0.9 MPa. Temperature evolution is also illustrated.

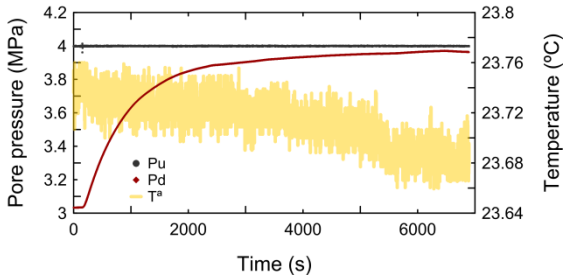

Figure 36. PPTM on a granite sample confined at hydrostatic pressure of 20 MPa. Initial upstream and incremental pressures of Pu~4 MPa and ΔP_0~1 MPa. Temperature evolution is also illustrated.

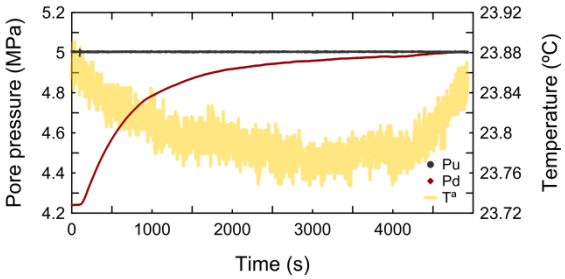

Figure 37. PPTM on a granite sample confined at hydrostatic pressure of 20 MPa. Initial upstream and incremental pressures of Pu~5 MPa and ΔP_0~0.8 MPa. Temperature evolution is also illustrated.

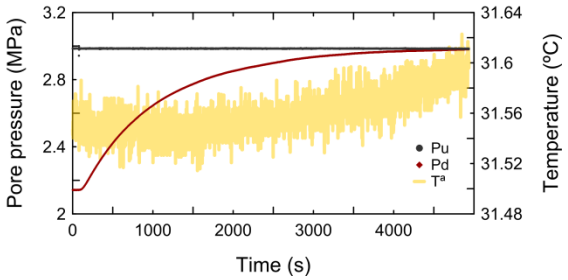

Figure 38. PPTM on a granite sample confined at hydrostatic pressure of 25 MPa. Initial upstream and incremental pressures of Pu~3 MPa and ΔP_0~0.9 MPa. Temperature evolution is also illustrated.

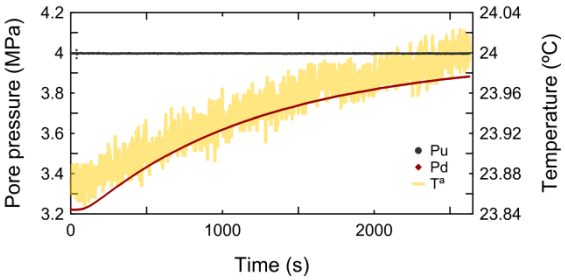

Figure 39. PPTM on a granite sample confined at hydrostatic pressure of 25 MPa. Initial upstream and incremental pressures of Pu~4 MPa and ΔP_0~0.8 MPa. Temperature evolution is also illustrated.